University of Dayton
eCommons

Chemical and Materials Engineering Faculty Publications

Department of Chemical and Materials Engineering

2014

Domain Engineering of Physical Vapor Deposited Two-Dimensional Materials

Tarek Alam
Pennsylvania State University - Main Campus

Baoming Wang
Pennsylvania State University - Main Campus

Raghu Pulavarthy
Pennsylvania State University - Main Campus

M. Amanul Haque
Pennsylvania State University - Main Campus

Christopher Muratore
University of Dayton, cmuratore1@udayton.edu

See next page for additional authors

Follow this and additional works at: https://ecommons.udayton.edu/cme_fac_pub

Part of the Other Chemical Engineering Commons, Other Materials Science and Engineering Commons, and the Polymer and Organic Materials Commons

Author(s)

Tarek Alam, Baoming Wang, Raghu Pulavarthy, M. Amanul Haque, Christopher Muratore, Nicholas R. Glavin, Ajit K. Roy, and Andrey A. Voevodin

Domain engineering of physical vapor deposited two-dimensional materials

Tarek Alam,[1] Baoming Wang,[1] Raghu Pulavarthy,[1] M. A. Haque,[1,a)] Christopher Muratore,[2] Nicholas Glavin,[3] Ajit K. Roy,[3] and Andrey A. Voevodin[3]

[1]*Department of Mechanical and Nuclear Engineering, The Pennsylvania State University, 314, Leonhard Building, University Park, Pennsylvania 16802, USA*
[2]*Kettering Laboratories, Department of Chemical and Materials Engineering, University of Dayton, Room 508A, Ohio 45469, USA*
[3]*Air Force Research Laboratory, Materials and Manufacturing Directorate, Wright Patterson AFB, 3005 Hobson Way, Building 651/253, Ohio 45433, USA*

Physical vapor deposited two-dimensional (2D) materials span larger areas compared to exfoliated flakes, but suffer from very small grain or domain sizes. In this letter, we fabricate freestanding molybdenum disulfide (MoS_2) and amorphous boron nitride (BN) specimens to expose both surfaces. We performed *in situ* heating in a transmission electron microscope to observe the domain restructuring in real time. The freestanding MoS_2 specimens showed up to $100\times$ increase in domain size, while the amorphous BN transformed in to polycrystalline hexagonal BN (h-BN) at temperatures around $600\,^\circ C$ much lower than the 850–$1000\,^\circ C$ range cited in the literature. © 2014 AIP Publishing LLC. [http://dx.doi.org/10.1063/1.4902937]

The rise of graphene[1] has galvanized the research on low dimensional materials that, to date, has extended to semiconducting transition metal di-chalcogenides (MoS_2 or WS_2) and insulating h-BN. This special class of materials consist of atomic layers with strong in-plane covalent bonding that are stacked together, with each layer bound by weak van der Waals bonding. The technological know-how from graphene has translated to other materials in 2D form and their intriguing layer/thickness dependence of thermophysical properties as well as novel phenomena such as spin, valley, or straintronics have led to the current resurgence of interest. For example, the indirect bandgap of bulk MoS_2 ($1.29\,eV$) shifts to direct type for a monolayer at $1.8\,eV$.[2] This gives rise to unprecedented interaction with light[3] that can be exploited in optoelectronic devices. Monolayers of MoS_2 in transistors show on/off ratios many orders of magnitude larger than the best graphene transistors at room temperature, with comparable mobility[4] and are aggressively pursued for electronic and optoelectronic devices.[5] A perfect foil for the semi-metal graphene is h-BN, also known as the *white graphene*, where atomically thick layers comprised of equal parts boron and nitrogen atoms form a 2D honeycomb structure iso-structural to graphite yet exhibiting very wide band gap of $5.9\,eV$ nearing an insulator and a very high in-plane thermal conductivity[6] around $390\,W\ m^{-1}\ K^{-1}$. Their low energy atomically smooth surfaces are free of dangling bonds as well as surface optical phonon modes, reducing phonon scattering from the dielectric. While these individual 2D materials are potentially interesting on their own, the exciting prospect of their stacking into heterostructures (or van der Waals' solids[7]) that currently propels 2D materials research. These are complex "on-demand designer materials" with controlled stacks of individual molecular or atomic layers building novel 3D materials with interesting structural, electronic, optical, mechanical, and other properties.[8]

The most influential microstructural parameter for 2D materials physics is the grain or domain boundaries, which reflects degree of laterally coherent atomic ordering within the material. Mechanical exfoliation of bulk crystals allows maintenance of a high degree of atomic-scale order in the transition from bulk to 2D when compared to vapor phase synthesis, but only over areas below $100\,\mu m^2$. As a result, exfoliated crystals make excellent specimens for fundamental research but are impractical for scaling up technological applications. Therefore, alternate techniques for large area growth using processes amenable to microelectronics, such as chemical or physical vapor deposition (CVD/PVD), have seen a major thrust in the literature. In this time, none of the large area synthesis processes has been able to produce exfoliation-grade results, primarily due to the domain boundaries. Chemical vapor deposition (CVD) of MoS_2, for example, results in triangular domains with size scale of few tens of microns. The growth of these domains is sensitive to the precursor gas concentration, and chamber pressure, while the nucleation rate dependence on extrinsic process parameters is yet to be understood and controlled. High surface energy features,[9] such as scratches, edges, as well as special precursor treatment[10] have been used to increase the nucleation site density. As a result, even though the individual triangles are highly crystalline, they physically overlap upon extended growth and form domain boundaries.[11] The presence of these overlaps critically influences the overall microstructure, which is obvious from the remarkable difference seen in the Raman spectra as a function of the number of monolayers.[12] The physical overlap of these crystallites increases nonlinearly with the number of layers; therefore, even though the individual domains can be large, the effective domain sizes are much smaller. PVD does not suffer from the isolated nucleation sites as CVD for continuous coverage, but in this case the crystallites are smaller. Hence,

---

a)Author to whom correspondence should be addressed. Electronic mail: mah37@psu.edu. Tel.: 814-865-4248. Fax: 814-865-9693.

the domain sizes are even smaller although the films demonstrate continuous coverage. Other large area synthesis processes, such as solution based dip-coating and thermolysis,[13] are also limited by such domain boundaries.

In this letter, we first highlight that atomic ordering of CVD, PVD, or solution based process is typically localized in individual domains or crystallites. Over larger areas, these isolated regions of highly ordered atoms are interrupted by domain boundaries, which generally degrades the properties of 2D materials.[9,10,14,15] Low temperature (200–300 °C) annealing is routinely done in the literature to eliminate surface contaminations or to improve the electrode contacts, for bulk and thin film materials but there is very little evidence of increased domain size of 2D materials, via post-process annealing. However, it was shown recently that a combination of localized and global heating results in *in-situ* annealing of high angle grain boundaries in chemical vapor deposited graphene.[16] While high temperature annealing is expected to induce such recrystallization of the grain boundaries, the required temperatures are too high for MoS_2 (Ref. 13) and BN.[17] MoS_2, for example, has been extensively used as high temperature (>700 °C) solid lubricant (in vacuum), while h-BN, which is less sensitive to the composition of the ambient environment, does not show substantial phase transformation (amorphous to crystalline) or grain size increase unless the temperature and pressure are very high (>1000 °C and 7.7 GPa).[18] Evidence in the literature for microstructural changes in h-BN thin films involves special catalysts[19] or lattice matched substrates,[20] such as ruthenium, with temperature exceeding 850 °C in either case. In air, annealing of MoS_2 results in layer thinning,[21] but most often complete oxidation at temperatures as low as 330 °C.[22] Sulfur desorption is sometimes observed at high temperatures under high vacuum.[23] Grain sizes of MoS_2 films do not increase beyond 10 nm (Ref. 24) even after annealing at 750 °C based on x-ray diffraction peaks and peak sharpening methods of the structure analysis. However, we also note that 2D materials are expected to be extremely sensitive to external stimuli, particularly because of the predominance of surface atoms which are also expected to have a higher mobility In this study, we expose both surfaces of the specimens by releasing them from the substrate. Our hypothesis is that doubling the number of highly mobile surface atoms (not to mention high energy features such as surface steps and ledges) will reduce the activation energy of atomic migration for domain reconstructions driven by a reduction of domain boundary energy. To test this hypothesis, we selected thicker (40 layer) MoS_2 and (10 layer) amorphous BN specimens. Thicker specimens are more robust for the pick-and-place technique for transferring films to devices used here, and also facilitate characterization for definitive evidence of structural effects. Moreover, it is anticipated that the recrystallization temperature increases with the specimen length-scale and hence thicker specimens pose a rigorous test of the proposed hypothesis. In this study, we adopt an *in-situ* transmission electron microscope (TEM) approach that is known to be effective in detecting precise changes in crystallinity through both imaging and electron diffraction modes.[25]

To examine the effects of heating of freestanding films, nanocrystalline MoS_2 (domain size around 5 nm) and

amorphous BN films were integrated into a micro-electro-mechanical system (MEMS) fitted with micro-heaters for *in situ* heating inside TEM. PVD techniques were used for growth of both materials on silicon substrates coated with 200 nm thick spin on glass. Briefly, the sputtering process involves generation of magnetically confined, cold, low pressure argon plasma adjacent to a pure MoS_2 disk. The disk also serves as the plasma cathode, driving positively charged argon ions into the disk, and liberating atoms from its surface. Those atoms condense on the substrate surface, where their kinetic energy and the substrate temperature dictate the resulting film microstructure. Asymmetric, bipolar voltage pulses were applied to the sputtering magnetron to control microstructure for surface plane (002) orientation.[26] BN films were deposited by pulsed laser deposition, where a focused laser beam pulse causes both ionized and neutral components from a BN target to accelerate to the desired substrate surface as a plasma plume in a nitrogen gas background. The deposition characteristics are controlled by laser wavelength, power, pulse rate, pulse duration, target-to-substrate working distance and relative orientation, background gas type and pressure, and substrate temperature. Previously, we have deposited few-layer MoS_2 and BN (mono to few-layers) on oxidized silicon substrates at temperatures as low as 350 °C and have performed complete characterization of the specimens.[27] A 10 nm titanium layer was deposited in the same PVD growth chamber to protect the BN and MoS_2 specimen layers without breaking the vacuum. This is shown in Figure 1(a), with inset elaborating the protective sandwich structure. In the next step, photolithography and reactive ion etching were used to pattern 10 μm wide and 100 μm long rectangular specimens that are released from the substrate. This step is shown in Figure 1(b). These sandwich (oxide-specimen-titanium) structures were then mechanically cleaved at the supporting ends and then manipulated on the MEMS device. Figure 1(c) shows this step with the cleaved specimen and the nanomanipulator needle in a focused ion beam (FIB) chamber.

Once the specimen is aligned with the MEMS device, it was secured with carbon deposition at the ends using a focused ion beam. The effective gage length of the specimen was about 10 μm. The MEMS device was then exposed to hydrofluoric acid vapor to remove the protective layers of spin on glass (SiO_2) and titanium without damaging the specimens. These two steps are shown in Figures 1(d) and 1(e), respectively. Energy filtered chemical element mapping confirmed removal of all traces of the Ti layer. No carbon was present either, suggesting that the specimen transfer technique is much cleaner than the conventional practice involving poly(methyl methacrylate).[28] Figure 1(f) shows an infrared image of the heaters integrated with the test chip. A finite element model was developed to calculate the temperature profile for heating at ambient conditions. The excellent agreement between the measurement and calculation is obvious from the overlap of these two lines. Next, the convective mode heat transfer was turned off in the model to estimate the temperature profile inside the TEM chamber.

Figure 2 shows the experimental results on the MoS_2 specimen. In as-deposited form, the microstructure was turbo-static as evident from the diffused rings in the electron
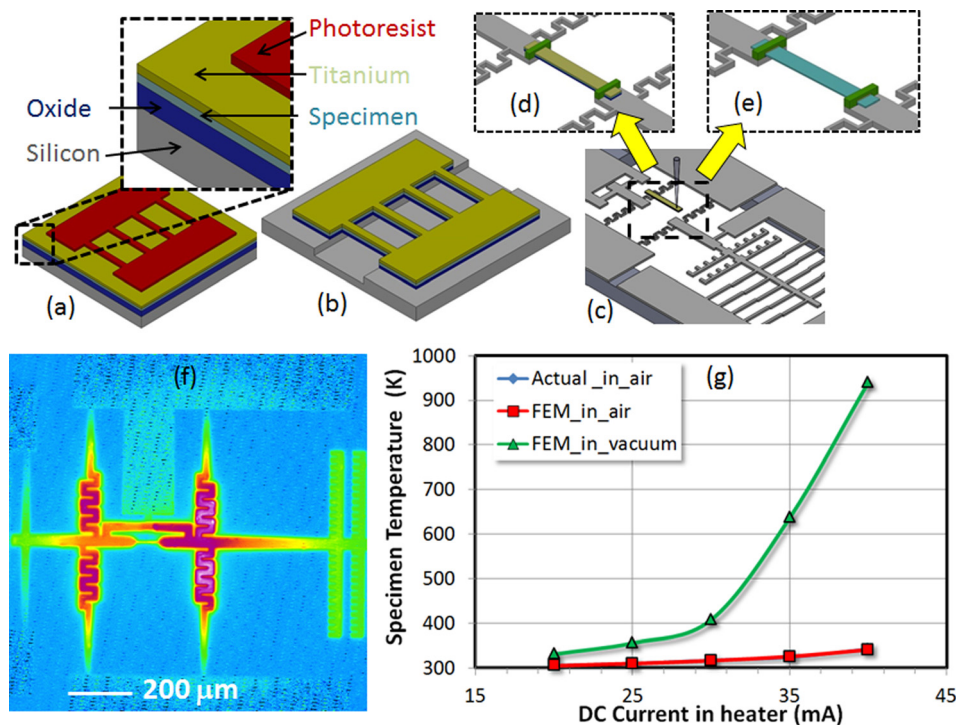
FIG. 1. Experimental details (a) PVD of specimen layers on oxide coated silicon wafer and a protective titanium over-layer, (b) reactive ion etching of all the layers and additional isotropic etching of silicon after photolithographic patterning preparation, (c) nano-manipulation of the a cleaved specimen on to a MEMS device and (d) securing it with carbon deposition, (e) vapor phase hydro-fluoric acid etch to remove the protective titanium and oxide layers, (f) infrared image of the MEMS heaters, and (g) experimental validation of a finite element model for heater temperature estimation in TEM.

diffraction pattern. High resolution TEM indicated average domain size around 3–5 nm. The Raman spectra clearly showed the signature peaks for stoichiometric MoS_2 but with reduced intensity indicative of phonon scattering over 5–10 nm domains. After annealing for 30 min at 600 °C, significant domain restructuring was observed as the average domain size increased to approximately 100 nm. Figure 2(d) shows a high resolution TEM image, where the lattice spacing of 0.61 nm clearly indicates crystalline phases of MoS_2, and the electron diffraction pattern shows spotty rings indicating grain growth. The effect of such low temperature and short time annealing is evident in Figure 2(f), where the Raman spectra of the annealed sample are compared with the as-deposited as well as a bulk single crystal of MoS_2. The comparison with the bulk crystal is very promising and

currently electrical measurements on the domain engineered specimens are underway.

While turbo-stratic to nanocrystalline phase transformation at relatively lower temperature in MoS_2 is remarkable, it is not energetically forbidden as seen in literature for carbonaceous materials albeit at higher temperatures.[29] A rather challenging and long lasting problem lies in amorphous specimens that typically require impractical magnitudes of temperature and pressure.[30] Figure 3 shows the experimental results with *in-situ* TEM annealing of the amorphous BN films at 600 °C for 30 min. The as-deposited amorphous boron nitride transformed into crystallites with average domain size of 100 nm. Indexing of the resulting electron diffraction pattern reveals a match with that for hexagonal structure of boron nitride, as shown in Figure 2(d). The transformed
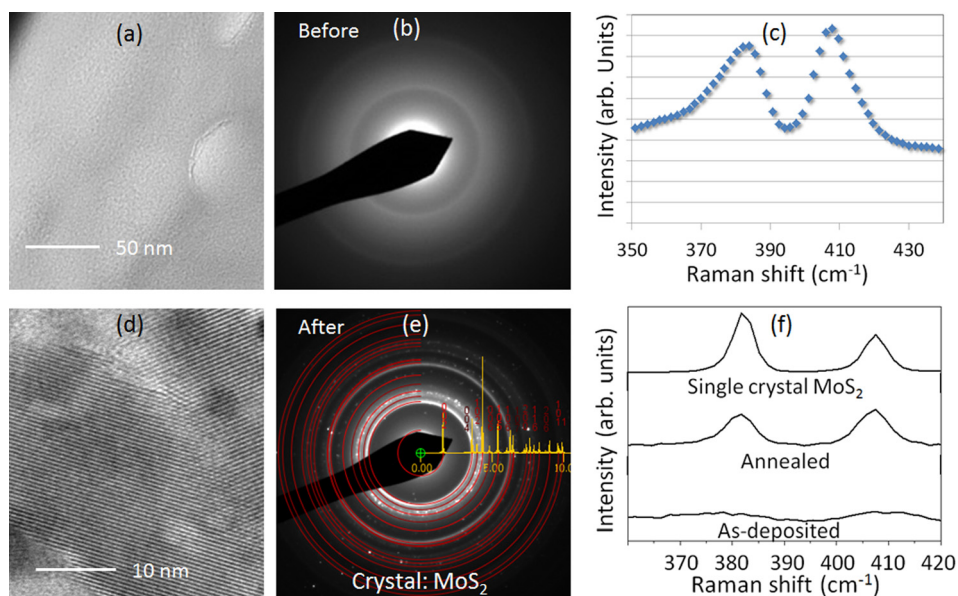

FIG. 2. Experimental results on MoS_2 (a) bright field TEM, (b) electron diffraction, and (c) Raman spectroscopy of the as-deposited specimen while supported on the substrate measured with 10 mW excitation laser power. After *in-situ* TEM annealing at 600 °C, (d) bright field TEM and (e) electron diffraction shows significant grain/domain growth, and (f) comparison of the as-deposited and annealed Raman spectra with that for a single crystal MoS_2. The power was reduced to 1 mW to avoid damage to the free-standing specimens, thus, the intensity of the as-deposited film is significantly reduced.
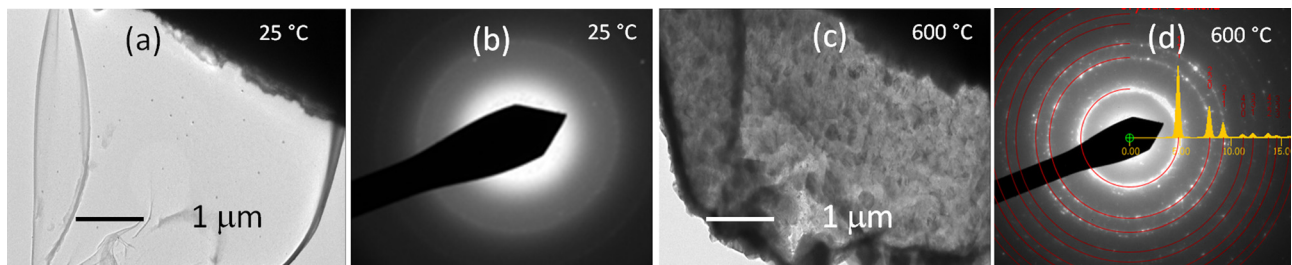
FIG. 3. Experimental results for amorphous boron nitride (a) bright field TEM and (b) electron diffraction of the as-deposited specimen. After *in-situ* TEM annealing at 600 °C, (d) bright field TEM and (e) electron diffraction shows significant grain/domain growth with hexagonal crystal structure.

structure was stable after the temperature was lowered to ambient.

To explain the observed phenomenon of grain growth in MoS_2 and the amorphous to nano-crystalline phase transformation in BN at only 600 °C, we note the dominant role of surface diffusion. In general, surface is the fastest pathway for atomic migration, which can be orders of magnitude higher than bulk and grain boundary diffusion.[31] Since the specimens in this study were freestanding, both surfaces provide a reduced activation energy for diffusion compared to specimens on substrates where the grain boundaries are essentially pinned or constrained by the substrate and even extremely high temperature is not effective in their migration towards grain growth. An extension of the present study under progress is quantification of the activation energy for grain or domain boundaries by measuring the grain sizes as function of temperature and time, carrying out the experiments for various thicknesses. The implications of our finding are two-fold: (i) provides an avenue for a large area synthesis of 2D materials by PVD methods with post-annealing; and (ii) experimental guidance to the concept of domain size engineering while using free surfaces to significantly reduce temperature requirements for structure restructuring activation. Successful implementation of domain engineering may allow us to grow these materials on any desired substrates and yet maintain acceptable crystallinity through post processing, relaxing the substrate constraint. However, domain size and grain-boundary defect engineering is mostly theoretical concept because study on grain boundaries in 2D materials is still at its infancy.[15] By maximizing domain size and minimizing boundary defect concentrations, it may be possible to achieve pristine-like performance in large area 2D materials, which is a dominant technological barrier for integration of this class of materials in diverse applications.

[1]A. K. Geim and K. S. Novoselov, Nat. Mater. **6**(3), 183 (2007).
[2]K. F. Mak, C. Lee, J. Hone, J. Shan, and T. F. Heinz, Phys. Rev. Lett. **105**(13), 136805 (2010).

[3]L. Britnell, R. M. Ribeiro, A. Eckmann, R. Jalil, B. D. Belle, A. Mishchenko, Y. J. Kim, R. V. Gorbachev, T. Georgiou, S. V. Morozov, A. N. Grigorenko, A. K. Geim, C. Casiraghi, A. H. C. Neto, and K. S. Novoselov, Science **340**(6138), 1311 (2013).
[4]B. Radisavljevic, A. Radenovic, J. Brivio, V. Giacometti, and A. Kis, Nat. Nanotechnol. **6**(3), 147 (2011).
[5]Y. Yoon, K. Ganapathi, and S. Salahuddin, Nano Lett. **11**(9), 3768 (2011); Q. H. Wang, K. Kalantar-Zadeh, A. Kis, J. N. Coleman, and M. S. Strano, Nat. Nanotechnol. **7**(11), 699 (2012).
[6]I. Jo, M. Thompson Pettes, J. Kim, K. Watanabe, T. Taniguchi, Z. Yao, and L. Shi, Nano Lett. **13**(2), 550 (2013).
[7]A. K. Geim and I. V. Grigorieva, Nature **499**(7459), 419 (2013).
[8]K. S. Novoselov and A. H. Castro Neto, Phys. Scr. **T146**, 014006 (2012); G. Gao, W. Gao, E. Cannuccia, J. Taha-Tijerina, L. Balicas, A. Mathkar, T. N. Narayanan, Z. Liu, B. K. Gupta, J. Peng, Y. Yin, A. Rubio, and P. M. Ajayan, Nano Lett. **12**(7), 3518 (2012); Y.-C. Lin, N. Lu, N. Perea-Lopez, J. Li, Z. Lin, X. Peng, C. H. Lee, C. Sun, L. Calderin, P. N. Browning, M. S. Bresnehan, M. J. Kim, T. S. Mayer, M. Terrones, and J. A. Robinson, ACS Nano **8**(4), 3715 (2014).
[9]S. Najmaei, Z. Liu, W. Zhou, X. Zou, G. Shi, S. Lei, B. I. Yakobson, J.-C. Idrobo, P. M. Ajayan, and J. Lou, Nat. Mater. **12**(8), 754 (2013).
[10]A. M. van der Zande, P. Y. Huang, D. A. Chenet, T. C. Berkelbach, Y. You, G.-H. Lee, T. F. Heinz, D. R. Reichman, D. A. Muller, and J. C. Hone, Nat. Mater. **12**(6), 554 (2013).
[11]Y.-H. Lee, X.-Q. Zhang, W. Zhang, M.-T. Chang, C.-T. Lin, K.-D. Chang, Y.-C. Yu, J. T.-W. Wang, C.-S. Chang, L.-J. Li, and T.-W. Lin, Adv. Mater. **24**(17), 2320 (2012).
[12]H. Li, Q. Zhang, C. C. Ray Yap, B. K. Tay, T. H. T. Edwin, A. Olivier, and D. Baillargeat, Adv. Funct. Mater. **22**(7), 1385 (2012).
[13]K.-K. Liu, W. Zhang, Y.-H. Lee, Y.-C. Lin, M.-T. Chang, C.-Y. Su, C.-S. Chang, H. Li, Y. Shi, H. Zhang, C.-S. Lai, and L.-J. Li, Nano Lett. **12**(3), 1538 (2012).
[14]Q. Yu, L. A. Jauregui, W. Wu, R. Colby, J. Tian, Z. Su, H. Cao, Z. Liu, D. Pandey, D. Wei, T. F. Chung, P. Peng, N. P. Guisinger, E. A. Stach, J. Bao, S.-S. Pei, and Y. P. Chen, Nat. Mater. **10**(6), 443 (2011).
[15]I. A. Ovidko, Rev. Adv. Mater. Sci. **30**, 201 (2012); available at: http://www.ipme.ru/e-journals/RAMS/no_33012/01_ovidko.pdf.
[16]J. Lee, J. Baek, G. Hee Ryu, M. J. Lee, S. Oh, S. K. Hong, B.-H. Kim, S.-H. Lee, B. J. Cho, Z. Lee, and S. Jeon, Nano Lett. **14**(8), 4352 (2014).
[17]M. S. Bresnehan, M. J. Hollander, M. Wetherington, K. Wang, T. Miyagi, G. Pastir, D. W. Snyder, J. J. Gengler, A. A. Voevodin, and W. C. Mitchel, J. Mater. Res. **29**(03), 459 (2014).
[18]K.-A. N. Duerloo, Y. Li, and E. J. Reed, Nat. Commun. **5**, 4214 (2014); T. Taniguchi, K. Kimoto, M. Tansho, S. Horiuchi, and S. Yamaoka, Chem. Mater. **15**(14), 2744 (2003).
[19]F. Liu, J. Yu, and X. Bai, Appl. Surf. Sci. **258**(24), 10191 (2012).
[20]P. Sutter, J. Lahiri, P. Zahl, B. Wang, and E. Sutter, Nano Lett. **13**(1), 276 (2013).
[21]J. Wu, H. Li, Z. Y. Yin, H. Li, J. Q. Liu, X. H. Cao, Q. Zhang, and H. Zhang, Small **9**(19), 3314 (2013).
[22]C. Muratore, J. E. Bultman, S. M. Aouadi, and A. A. Voevodin, Wear **270**(3–4), 140 (2011).
[23]M. Donarelli, F. Bisti, F. Perrozzi, and L. Ottaviano, Chem. Phys. Lett. **588**(0), 198 (2013).
[24]S. K. Ghosh, C. Srivastava, S. Nath, and J.-P. Celis, Int. J. Electrochem. **2013**, 1.
[25]S. Simões, R. Calinas, M. T. Vieira, M. F. Vieira, and P. J. Ferreira, Nanotechnology **21**(14), 145701 (2010).
[26]C. Muratore and A. A. Voevodin, Thin Solid Films **517**(19), 5605 (2009).

[27]C. Muratore, J. J. Hu, B. Wang, M. A. Haque, J. E. Bultman, M. L. Jespersen, P. J. Shamberger, M. E. McConney, R. D. Naguy, and A. A. Voevodin, Appl. Phys. Lett. **104**(26), 261604 (2014); N. R. Glavin, M. L. Jespersen, M. H. Check, J. Hu, A. M. Hilton, T. S. Fisher, and A. A. Voevodin, "Synthesis of few-layer, large area hexagonal-boron nitride by pulsed laser deposition," Thin Solid Films (published online).

[28]Y.-C. Lin, C.-C. Lu, C.-H. Yeh, C. Jin, K. Suenaga, and P.-W. Chiu, Nano Lett. **12**(1), 414 (2012).

[29]C. M. Lentz, B. A. Samuel, H. C. Foley, and M. A. Haque, J. Nanomater. **2011**, 129298.

[30]G. C. Loh and D. Baillargeat, J. Appl. Phys. **114**(3), 033534 (2013).

[31]G. Antczak and G. Ehrlich, *Surface Diffusion: Metals, Metal Atoms, and Clusters* (Cambridge University Press, Cambridge, UK, 2010).